MJFAS
Malaysian Journal of Fundamental and Applied Sciences

Hoong and Hoe | Malaysian Journal of Fundamental and Applied Sciences, Vol. 18 (2022) 343-366

RESEARCH ARTICLE

Modeling of Traffic Flow on Roundabouts

Cheah Yuat Hoong[a,b,*], Yeak Su Hoe[a]

[a] Department of Mathematical Sciences, Faculty of Science, Universiti Teknologi Malaysia, 81310 UTM, Johor Bahru, Malaysia; [b] Xiamen University Malaysia, Jalan Sunsuria, Bandar Sunsuria, 43900 Sepang, Selangor, Malaysia.

Abstract The aim of this research is to create the modeling of roundabouts. First of all, the three-arm roundabout is created for validation with the existing model. Then, the model is expanded to the four-arm roundabout. In the development of a modern intelligent transportation system, the effectiveness of dealing with the non-linear, time-varying and congested traffic flow is imperative in achieving traffic control and accuracy. In this paper, the roundabout is modelled as a circuit of 2×2 junction comprising a main lane and a secondary lane. The rotation of the roundabout is in the clockwise direction, as in the case of Malaysia. In mathematical modelling, the traffic flow is created, based on one-dimensional hyperbolic conservation laws which are represented by non-linear partial differential equations where the unknown variable is a conserved quantity. As a scheme used in the computation and analysis, the Godunov method computes the fluxes at the interfaces of each cell in order to advance the solution of a Riemann Problem. In addition, the Courant-Friedrichs-Levy (CFL) condition is proposed and used to ensure the stability and accuracy of the numerical algorithm where the time step is not a constant. The optimization on the roundabout for Total Travel Time and Total Waiting Time with several parameters is applied to generate numerous results which will assist in assessing the reasonableness of the roundabout. The comparison data of the three-arm roundabout with our model and the existing model are discussed. In comparison, our results show similar properties with higher readings than in other published papers because our calculations involved all arms and roads. In addition, the comparison data between three-arm and four-arm roundabouts are reasonable and logical. Lastly, our model is more flexible and realistic, as compared to the existing model.

Keywords: Traffic flow, Hyperbolic Conservation Laws, Godunov Method, CFL condition.

Introduction

Nowadays, the increasing congestion of roads in Malaysia is a cause for concern. According to an online survey conducted by global carmaker Ford, most Malaysians complained of road congestion as it made them spend more time and money on their daily transportation compared to a year ago. Data from the Malaysian Road Transport Department (JPJ) show that there are 2.59 million units of motor vehicles registered in Malaysia between 2016 and 2020. This figure represents an average increase of around 519.000 new vehicles annually in the past 5 years. Among the reasons attributed to road congestion, one of them is the construction of junctions and traffic lights. Hence, the situation results in a delayed response. Congestion on the road is a continuously growing problem that is said to cause degradation in terms of travel time, traffic safety, fuel consumption and environmental pollution [1].

One of the initiatives in reducing the congestion problem involves the introduction of the roundabout. Typically, the roundabout could transfer a complicated junction into several T-junctions as well as reduce speed [2]. It provides an alternative to the conventional junction by reducing the number of

***For correspondence:**
y_hoong0617@yahoo.com

Received: 18 Sept 2021
Accepted: 26 June 2022

traffic flow junctions. Roundabouts can significantly increase the smoothness of traffic flow through a multiple-road junction, both in terms of throughput and safety.

Research to study a simulation scheme for traffic flow is needed, and a comprehensive survey of vehicle dynamics within a mathematical framework should be developed. A large number of research studies have focused on the area of simulating vehicle interaction and driver behavior to understand how new rules and regulations could help relieve heavy road congestion. Given that the advantages of the roundabout are clearly defined, we are able to create a modeling of roundabout and study its optimization. Firstly, in order to create a four-arm roundabout model, the three-arm roundabout model must be created and validated with the existing model. In 2015, Obsu created a three -arm roundabout model [3]. However, in the calculation of Total Travel Time and Total Waiting Time, the author only considered a single-arm junction with two incoming roads and two outgoing roads. Nevertheless, our calculation will involve all the arm junctions with six incoming roads and six outgoing roads. After that, we will make a comparison and analysis of our results with Obsu's findings, as well as with the four-arm roundabout. The Total Travel Time and Total Waiting Time are calculated, based on the travelling time by drivers and the queue time on buffers, respectively.

Supposedly, there are two types of scales of traffic simulation in terms of a basic understanding for simulating traffic, namely, microscopic and macroscopic [4]. For this research, we create the model based on macroscopic and hyperbolic conservation laws. The first major step in the macroscopic modelling of traffic flow was undertaken by Lighthill and Whitham in 1955, when they indexed the comparability of traffic flow on long crowded roads with 'flood movements in long rivers'. A year later, Richards (1956) complemented the idea with the introduction of 'shock-waves on the highway', completing the so-called Lighthill-Whitham-Richards (LWR) model [3]. This LWR model proposed a fluid dynamic model for traffic flow on a single lane using nonlinear partial differential equations. In our simulation, the density is a factor.

Our study will use the Godunov method to solve the non-linear partial differential equations in the designated traffic-flow field because this method has been widely adopted by many researchers. This is based on the 1999 study by Sweby to approximate the solution of hyperbolic conservation laws, since this method can be characterized by the exact solution or approximated solution of a Riemann Problem within computational cells in order to obtain the numerical fluxes [5]. Moreover, this method has also been presented by Sonnendrucker in 2013 to solve the hyperbolic problem [6]. In 2014, the research on the optimization on roundabouts conducted by Obsu [3] was presented as a method to solve this problem.

Traffic Flow on Roundabouts

In general, most of the roundabouts have four incoming and four outgoing flow directions. In this research, the three-arm roundabout is created to compare with Obsu's model. This model has also been expanded to a four-arm roundabout. In fact, the incoming vehicles entering the roundabout can exit at any four outgoing roads by making an appropriate turning around the central island of roundabouts in a clockwise direction. Hence, several parameters are set, as similar to Obsu's model, which will help monitor the number of cars on the incoming secondary lane, those on the outgoing secondary lane, and also the number of cars passing through the arm junction from the incoming main lane and moving towards the outgoing main lane.

Traffic Flow Model

The model of traffic flow is based on the hyperbolic conservation laws that are non-linear partial differential equations where the unknown variable is a conserved quantity. Hence, the conservation of cars described by a first-order partial differential equation in one-dimensional form

$$\partial_t \rho + \partial_x f(\rho) = 0 \tag{1}$$

where $\rho = \rho(x,t)$ is the density of cars, with $\rho \in [0,\ \rho_{max}]$, $(x,t) \in \mathbb{R}^2$, with x is one-dimensional space variable and t is time variable and ρ_{max} is the maximum density of cars on the road, $f(\rho)$ is flux function and it can be written as $f(\rho) = \rho v(\rho)$, where $v(x,t)$ is the velocity.

In modeling, the design of traffic flow of cars on the road is usually a one-dimensional travel lane where overtaking is not possible. The unit measurement of $\rho(x,t)$ denotes the number of cars per unit length in $x \in \mathbb{R}$ at time, $t \geq 0$. The number of cars in the interval (x_1, x_2) at time t is

$$\int_{x_1}^{x_2} \rho(x,t)\, dx \tag{2}$$

Let $v(x,t)$ denote the velocity of cars in x at time t. Hence, the number of cars that will pass through x at time t (in unit length) is $\rho(x,t)v(x,t)$. The derivation of an equation for evolution of car density is the number of cars in the interval (x_1, x_2) changes according to the number of cars that enter and leave this interval, hence the assumption is made that no cars can be created or destroyed in this interval.

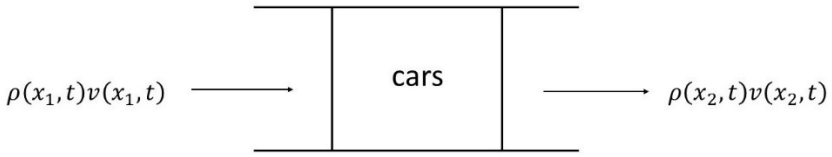

Figure 1. Derivation of the conservation law.

The number of cars in the interval (x_1, x_2) over a period of time is

$$\frac{d}{dt}\int_{x_1}^{x_2} \rho(x,t)\, dx = \rho(x_1,t)v(x_1,t) - \rho(x_2,t)v(x_2,t) \tag{3}$$

where the left-hand side of the Equation 3 is

$$\frac{d}{dt}\int_{x_1}^{x_2} \rho(x,t)\, dx = \int_{x_1}^{x_2} \frac{\partial \rho}{\partial t} dx \tag{4}$$

This is a global conservation law for vehicles on the road. If $\rho(x_2,t)v(x_2,t) > \rho(x_1,t)v(x_2,t)$, this represents more cars moving out from this interval, and yields the decreasing number of cars in the interval.

Integrating Equation 3 with respect to time, t and assuming that ρ and v are regular functions yields

$$\int_{t_1}^{t_2}\int_{x_1}^{x_2} \partial_t \rho(x,t)\, dx\, dt = \int_{t_1}^{t_2} [\rho(x_1,t)v(x_1,t) - \rho(x_2,t)v(x_2,t)]\, dt \tag{5}$$

By using the fundamental theorem of calculus, the right-hand side of the Equation 5 is

$$\int_{t_1}^{t_2} [\rho(x_1,t)v(x_1,t) - \rho(x_2,t)v(x_2,t)]\, dt = -\int_{t_1}^{t_2}\int_{x_1}^{x_2} \partial_x\, [\rho(x,t)v(x,t)] dx\, dt \tag{6}$$

Since $x_1, x_2 \in \mathbb{R},\ t_1, t_2 > 0$ are arbitrary, the Equation 5 can be concluded as,

$$\rho_t + (\rho v)_x = 0\ , x \in \mathbb{R}, t > 0 \tag{7}$$

This is a partial differential equation of first-order and can be classified as inviscid Burger's equation which can develop discontinuities or shock waves [7].

In Equation 7, the expression ρv can be treated as a flux function, $f(\rho) = \rho v$ can be represented by the

flux of cars, which is a product of the density and speed of cars. Often, at the first-order approximation, the assumption is that v is a decreasing function of ρ, hence flux is a concave function. This model is known in traffic literature as the Lighthill-Whitham-Richards (LWR) model. The main assumption of the Lighthill-Whitham-Richards model is that the velocity depends on the density of cars only because v is a decreasing function of the density [8].

Roundabout Model

In this research, a roundabout with four arms is considered as the study where the traffic flow in the roundabout is in a clockwise direction, as in Figure 2.

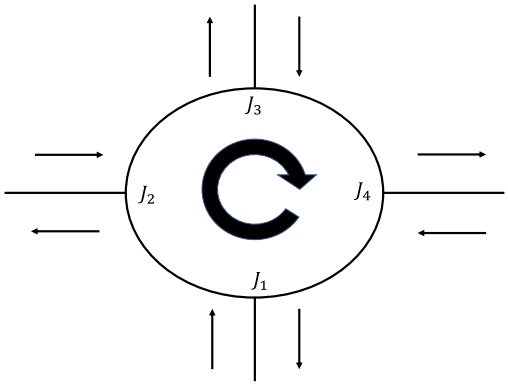

Figure 2. Sketch of roundabout.

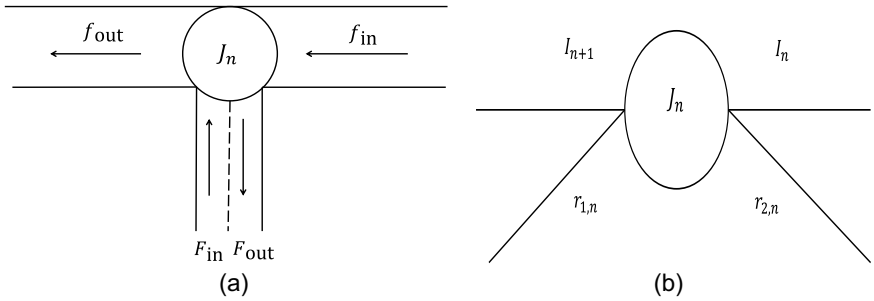

Figure 3. (a) Arm junction of roundabout. (b) Corresponding arm junction.

In Figure 2, the arm junction of roundabout $J_n, n = 1, 2, 3, 4$ can be interpreted as a 2×2 circuit arm junction where main lane, I and secondary lane, r are described by arcs and arm junctions by vertexes. Each arm junction is partitioned by an interval $[I_n, I_{n+1}], n = 1, 2, 3, 4$ and the periodic boundary condition is $I_5 = I_1$. The number of secondary lanes corresponds with the number of arms of the roundabout, and it consists of both incoming and outgoing roads. The details of networks are shown in Figure 3.

The traffic flow on the main lane segment is derived from Equation 1.

$$\partial_t \rho_n + \partial_x f(\rho_n) = 0, (x, t) \in \mathbb{R}^+ \times I_n, n = 1, 2, 3, 4 \tag{8}$$

For the above equation, $\rho_n = \rho_n(x, t) \in [0, \rho_{\max}]$ is the mean traffic density, $\rho_{\max}$ is the maximal density on road and the flux function $f: [0, \rho_{\max}] \to \mathbb{R}^+$ is given by the flux-density relation.

$$f(\rho) = \begin{cases} \rho v_{\max} & , 0 \le \rho \le \rho_c \\ \frac{f^{\max}}{\rho_{\max} - \rho_c}(\rho_{\max} - \rho) & , \rho_c \le \rho \le \rho_{\max} \end{cases} \tag{9}$$

In Equation 9, $v_{\max}$ is the maximal traffic speed, $\rho_c = \frac{f^{\max}}{v_{\max}}$ is the critical density and $f^{\max} = f(\rho_c)$ is the maximal flux value. For simplicity, some fixed constants are $\rho_{\max} = 1$ and $v_{\max} = 1$.

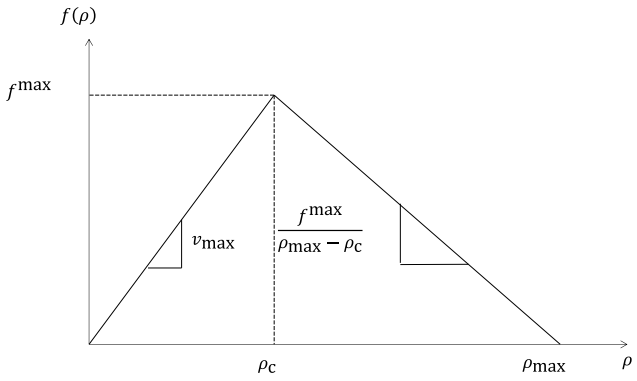

Figure 4. The rational flux-density relation graph.

To be realistic, the flux of the secondary lane entering the arm junction is assigned with a buffer of infinite size and capacity so as to prevent backward moving shocks on the road. In fact, the queue length of each buffer on the secondary lane is represented by ordinary differential equations.

$$\frac{dl_n(t)}{dt} = F_{\text{in}}^n(t) - \gamma_{\text{r1},n}(t), t \in \mathbb{R}^+, n = 1,2,3,4 \tag{10}$$

For the lane equation, $l_n(t) \in [0, +\infty]$ is the queue length, $F_{\text{in}}^n(t)$ is the flux entering the secondary lane and $\gamma_{\text{r1},n}(t)$ is the flux exiting the secondary lane and entering the roundabout. For simplicity, the outgoing lane on the secondary lane accepts all the fluxes coming out from the roundabout.

The Cauchy problem on the arm junction is,

$$\begin{cases} \partial_t \rho_n + \partial_x f(\rho_n) = 0, \quad (x,t) \in \mathbb{R}^+ \times I_n \\ \frac{dl_n(t)}{dt} = F_{\text{in}}^n(t) - \gamma_{\text{r1},n}(t), \quad t \in \mathbb{R}^+ \\ \rho_n(x,0) = \rho_{n,0}(x), \quad \text{on } I_n \\ l_n(0) = l_{n,0} \end{cases} \tag{11}$$

for $n = 1,2,3,4$ where $\rho_{n,0}(x)$ refers to the initial densities and $l_{n,0}$ will be the initial length.

Furthermore, some flux conditions on the secondary lane will be taken into account with the Cauchy problem above. They are demand $d(F_{\text{in}}^n, l_n)$ on the incoming secondary lanes, the demand function $\delta(\rho_n)$ on the incoming main lanes, and the supply function $\sigma(\rho_n)$ on the outgoing main lanes at each arm junction.

$$d(F_{\text{in}}^n, l_n) = \begin{cases} \gamma_{\text{r1},n}^{\max} & , l_n(t) > 0 \\ \min\left(F_{\text{in}}^n(t), \gamma_{\text{r1},n}^{\max}\right) & , l_n(t) = 0 \end{cases} \tag{12}$$

$$\delta(\rho_n) = \begin{cases} f(\rho_n) & , 0 \le \rho_n < \rho_c \\ f^{\max} & , \rho_c \le \rho_n \le 1 \end{cases} \tag{13}$$

$$\sigma(\rho_n) = \begin{cases} f^{\max} & , 0 \le \rho_n \le \rho_c \\ f(\rho_n) & , \rho_c < \rho_n \le 1 \end{cases} \tag{14}$$

for $n = 1, 2, 3, 4$ where $\gamma_{\mathrm{r1},n}^{\max}$ is the maximal flow on the incoming secondary lanes $r_{1,n}$. In addition, $\beta \in [0, 1]$ is the supply ratio of the outgoing secondary lanes $r_{2,n}$ and its flux

$$\gamma_{\mathrm{r2},n}(t) = \beta_n f\big(\rho_n(0-,t)\big), n = 1, 2, 3, 4 \tag{15}$$

The flux on the arm junction can be classified by both the incoming and outgoing flux. The flux of the outgoing main lane is subjected to

$$f\big(\rho_{n+1}(0+,t)\big) = \min\Big((1-\beta_n)\delta\big(\rho_n(0-,t)\big) + d\big(F_{\mathrm{in}}^n(t), l_n(t)\big), \sigma\big(\rho_{n+1}(0+,t)\big)\Big) \tag{16}$$

Meanwhile, the flux from the incoming main lane is subjected to

$$f\big(\rho_n(0-,t)\big) = f\big(p_{n+1}(0+,t)\big) + \gamma_{\mathrm{r2},n}(t) - \gamma_{\mathrm{r1},n}(t) \tag{17}$$

where $n = 1, 2, 3, 4$.

Riemann Problem and Riemann Solver at Arm Junction

The Riemann problem at arm junction is the Cauchy problem in Equation 11 where the initial conditions are given by $\rho_{n,0}(x) = \rho_{n,0}$ on I_n for $n = 1, 2, 3$ and 4 in which each arm junction has an incoming road and an outgoing road. Some constants can be fixed likely $\rho_{n,0} \in [0, 1], l_{n,0} \in [0, \infty), F_{\mathrm{in}}^n \in (0, \infty)$ and priority factor $P_n \in (0, 1)$. Riemann Solver is constructed as follows:

- Define $\Gamma_{1_n}^t = f\big(\rho_n(0-,t)\big), \Gamma_{2_n}^t = f\big(\rho_{n+1}(0+,t)\big), \Gamma_{\mathrm{r1}_n}^t = \gamma_{\mathrm{r1}}(t)$.
- Consider the space $\big(\Gamma_{\mathrm{r1}_n}^t, \Gamma_{1_n}^t\big)$ and the sets
$$\varphi_1 = \big[0, \delta\big(\rho_{n,t}\big)\big], \varphi_{\mathrm{r1}} = [0, d(F_{\mathrm{in}}^n(t), l_n(t))].$$
- Trace the lines $(1-\beta_n)\Gamma_{1_n}^t + \Gamma_{\mathrm{r1}_n}^t = \Gamma_{2_n}^t$ and $\Gamma_{1_n}^t = \frac{P_n}{(1-P_n)(1-\beta_n)}\Gamma_{\mathrm{r1}_n}^t$.
- Consider the region
$$\Omega = \big\{\big(\Gamma_{\mathrm{r1}_n}^t, \Gamma_{1_n}^t\big) \in \varphi_1 \times \varphi_{\mathrm{r1}} : (1-\beta_n)\Gamma_{1_n}^t + \Gamma_{\mathrm{r1}_n}^t \in \big[0, \Gamma_{2_n}^t\big]\big\}.$$

Riemann Solver at two situations depends on the value of Γ_2:

- Demand-limited case: $\Gamma_{2_n}^t = (1-\beta_n)\delta\big(\rho_{n,t}\big) + d(F_{\mathrm{in}}^n(t), l_n(t))$

Set $\Gamma_{1_n}^t = \delta\big(\rho_{n,t}\big)$ and $\Gamma_{\mathrm{r1}_n}^t = d(F_{\mathrm{in}}^n(t), l_n(t))$ in Figure 5 (a).

- Supply-limited case: $\Gamma_{2_n}^t = \sigma\big(\rho_{n+1,t}\big)$

Set Q which is the point of intersection of $(1-\beta_n)\Gamma_{1_n}^t + \Gamma_{\mathrm{r1}_n}^t = \Gamma_{2_n}^t$ and $\Gamma_{1_n}^t = \frac{P_n}{(1-P_n)(1-\beta_n)}\Gamma_{\mathrm{r1}_n}^t$. If $Q \in \Omega$, set $\big(\Gamma_{\mathrm{r1}_n}^t, \Gamma_{1_n}^t\big) = \mathrm{Q}$ in Figure 5(b). Otherwise, $Q \notin \Omega$, set $\big(\Gamma_{\mathrm{r1}_n}^t, \Gamma_{1_n}^t\big) = S$ where S is the point of segment $\Omega \cap \big(\Gamma_{\mathrm{r1}_n}^t, \Gamma_{1_n}^t\big) : (1-\beta_n)\Gamma_{1_n}^t + \Gamma_{\mathrm{r1}_n}^t = \Gamma_{2_n}^t$ closest to the line $\Gamma_{1_n}^t = \frac{P_n}{(1-P_n)(1-\beta_n)}\Gamma_{\mathrm{r1}_n}^t$ in Figure 5(c).

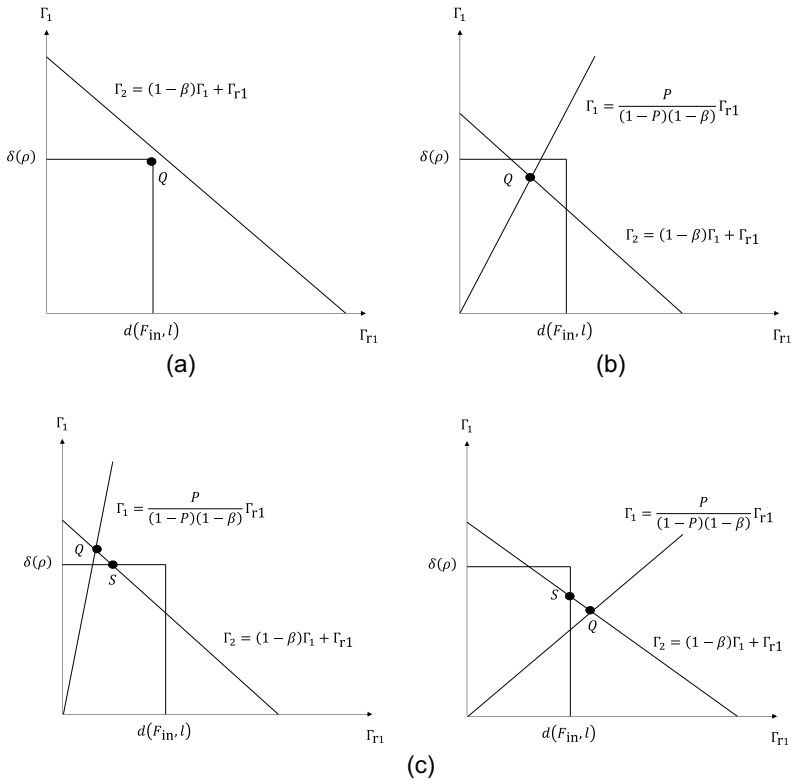

Figure 5. (a) Demand-limited case. (b) Supply-limited case – intersection inside Ω. (c) Supply-limited case – intersection outside Ω.

Network Topology

The roundabout with four arms is modeled by four main roads, namely, I_1, I_2, I_3 and I_4. Each main road is divided by i node points and form $(i+1)$ intervals. It has a secondary lane on each arm junction with an incoming road and an outgoing road. The overall traffic flow runs on a single lane and unsignalized. In other words, there will be no overtaking of cars. From this topology, it can be shown that all the arm junctions of the roundabout can be represented by a circuit of 2×2 junction.

Numerical Scheme

According to the topology, a numerical grid is in $J_n \leq x \leq J_{n+1}$ and $0 \leq t \leq T$ using the following notation:

- Δ_x is the space grid size.
- Δt^j is the inconstant time grid size.
- $(x_i, t^j) = (i\Delta_x, t^{j-1} + \Delta t^j)$ for $i \in \mathbb{Z}$ and $j \in \mathbb{N}$ are the gird points.

Godunov Method

We used the Godunov method to compute the flux at each cell interface because this method explores piecewise constant solutions as the solution is propagating at a finite speed and can be computed exactly by solving a Riemann problem.

The finding of the solution is designed in rectangle mesh where $J_n \leq x \leq J_{n+1}$ and $0 \leq t \leq T$. In fact, the grid is defined as

$$x_i = J_n + \left(i + \frac{1}{2}\right)h, \quad i = 1, 2, 3, \ldots, M$$

$$t^j = (j-1)k, \;\; j = 1, 2, 3, \ldots, N+1$$

Each sub-interval is distributed as $[J_n, J_n + h], [J_n + h, J_n + 2h], \ldots, [J_{n+1} - h, J_{n+1}]$ cells. The points x_i are the midpoints of these cells, and the ith cell is $\left[x_i - \frac{h}{2}, x_i + \frac{h}{2}\right]$ and is given by $C_{i,j} = \left[x_{i-\frac{1}{2}h,j}, x_{i+\frac{1}{2}h,j}\right]$ at time t^j. The Godunov scheme is a first-order scheme that is characterized as an exact solution to the Riemann problem.

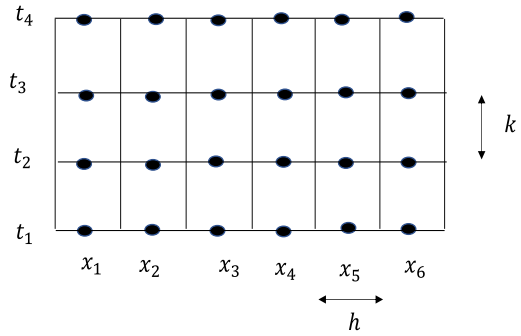

Figure 6. The mesh grids.

Instead of directly approximating ρ at each of the grid points, the approximation of the average of ρ over each cell is

$$u_{i,j} = \frac{1}{h}\int_{x_{i-\frac{h}{2}}}^{x_{i+\frac{h}{2}}} \rho(x, t_j)\, dx \tag{18}$$

The average cell change over one-time step can be obtained by replacing the Equation 5 as in

$$x_1 = x_{i-\frac{1}{2}h}, x_2 = x_{i+\frac{1}{2}h}, t_1 = t_j, t_2 = t_{j+1}$$

Hence,

$$\int_{x_{i-\frac{1}{2}h}}^{x_{i+\frac{1}{2}h}} \rho(x, t_{j+1})\, dx - \int_{x_{i-\frac{1}{2}h}}^{x_{i+\frac{1}{2}h}} \rho(x, t_j)\, dx = \int_{t_j}^{t_{j+1}} f\left(\rho\left(x_{i-\frac{1}{2}h}, t\right)\right) - f\left(\rho\left(x_{i+\frac{1}{2}h}, t\right)\right) dt \tag{19}$$

Divide Equation 19 by h,

$$u_{i,j+1} - u_{i,j} = \frac{1}{h}\int_{t_j}^{t_{j+1}} f\left(\rho\left(x_{i-\frac{1}{2}h}, t\right)\right) dt - \frac{1}{h}\int_{t_j}^{t_{j+1}} f\left(\rho\left(x_{i+\frac{1}{2}h}, t\right)\right) dt$$

$$u_{i,j+1} = u_{i,j} - \frac{k}{h}\left(f\left(\rho\left(x_{i+\frac{1}{2}h}, j\right)\right) - f\left(\rho\left(x_{i-\frac{1}{2}h}, j\right)\right)\right) \tag{20}$$

The intersection of waves between two neighboring cells takes place from the determination of Δt^j by the CFL (Courant-Friedrichs-Lewy) condition.

$$\Delta t^j \max\left|\lambda^j_{i+\frac{1}{2}h}\right| \leq \frac{1}{2}\Delta x, \text{where } i \in \mathbb{Z} \text{ and } j \in \mathbb{N} \tag{21}$$

In Equation 21, $\lambda^j_{i+\frac{1}{2}h}$ is the wave speed at the interface $x_{i+\frac{1}{2}h}$ at time t^j and is defined as $f'(u)$. Based on the condition in Equation 21, the scheme can be written as

$$u_i^{j+1} = u_i^j - \frac{\Delta t^j}{\Delta x}\left(G\left(u_i^j, u_{i+1}^j\right) - G\left(u_{i-1}^j, u_i^j\right)\right) \tag{22}$$

where the $G\left(u_i^j, u_{i+1}^j\right) = G^j_{i+\frac{1}{2}}$ is the Godunov numerical flux given by

$$G(x, y) = \begin{cases} \min\left(f(x), f(y)\right) & \text{if } x \le y \\ f(x) & \text{if } y < x < \rho_c \\ f^{\max} & \text{if } y < \rho_c < x \\ f(y) & \text{if } \rho_c < y < x \end{cases} \tag{23}$$

However, the conditions at arm junction, for the incoming main lane, are

$$u_i^{j+1} = u_i^j - \frac{\Delta t^j}{\Delta x}\left(\Gamma_1{}^j_n - G\left(u_{i-1}^j, u_i^j\right)\right) \tag{24}$$

and for the outgoing main lane,

$$u_i^{j+1} = u_i^j - \frac{\Delta t^j}{\Delta x}\left(G\left(u_i^j, u_{i+1}^j\right) - \Gamma_2{}^j_n\right) \tag{25}$$

where Γ_1 and Γ_2 are the maximized fluxes computed in the Riemann Problem and Riemann Solver at Arm Junction section.

Lane

The buffer modeled in Equation 10 is the entrance at the junction of the roundabout. At each time step $t^j = t^{j-1} + \Delta t^j$, the new queue value length for $t^{j+1}i$ is computed according to the two possible cases with Euler first-order integration [9].

- If $F_{\text{in}}\left(t^j\right) < \Gamma_{\text{r1}}{}^j_n$

$$l_n^{j+1} = \begin{cases} l^j + \left(F_{\text{in}}(t^j) - \Gamma_{\text{r1}}{}^j_n\right)\Delta t^j & \text{for } t^{j+1} < \bar{t}, \\ 0 & \text{otherwise,} \end{cases} \tag{26}$$

- If $F_{\text{in}}\left(t^j\right) > \Gamma_{\text{r1}}{}^j_n$

$$l_n^{j+1} = l^j + \left(F_{\text{in}}(t^j) - \Gamma_{\text{r1}}{}^j_n\right)\Delta t^j \tag{27}$$

In Equations 26 and 27, $\Gamma_{\text{r1}}{}^j_n$ is the maximized flux computed in the Riemann Problem and Riemann Solver at Arm Junction section and $F_{\text{in}}\left(t^j\right)$ is the flux entering the entrance of the roundabout at time t^j given by

$$F_{\text{in}}(t^j) = \frac{1}{\Delta t^j}\int_{t^j}^{t^{j+1}} F_{\text{in}}(t)\, dt \tag{28}$$

and $\bar{t}$ is the empty buffer time. Calculate it for each time step Δt^j.

$$\bar{t} = -\frac{l^j}{F_{\text{in}}(t^j) - \Gamma_{\text{r1}}{}^j_n} + t^j \tag{29}$$

Numerical Simulations Setting

In conducting the simulation, some parameters must be taken into account to yield more realistic results which have been introduced in the "Traffic Flow on Roundabouts' section where $F_{\text{in}} \in [0,1]$, $\beta \in [0,1]$ and $P \in [0,1]$. For validation purposes, the initial conditions are set as in Obsu's paper, and it is very likely that at the initial time, all the roads and the buffers are empty, $\rho_{n,0} = 0$, $F_{\text{in}}^{n} \neq 0$ and $l_{n,0} = 0$ where $n = 1, 2, 3$ and 4. These are very realistic. Also, some constants are $f^{\max} = 0.66$, $\rho_c = 0.66$ and $\gamma_{\text{r1}}^{\max} = 0.65$. Lastly, the total time and space step are $T = 50$ and $\Delta x = 0.1$, respectively. In our simulation, we set the various settings; for instance, the circumference of the roundabout is set to three unit lengths and four unit lengths. In addition, the setting of F_{in}^{n}, P_n and β_n on each arm is distinct.

Optimization on Roundabout

In order to study the reasonableness and logic of the roundabout model, the calculations of Total Travel Time (TTT) on the road network and Total Waiting Time (TWT) at the entrance of the secondary road have to be calculated. The Total Travel Time and Total Waiting Time of the three-arm roundabout are compared with Obsu's results. As mentioned in the introduction of this paper, the calculation is based on a single-arm junction with two incoming roads and two outgoing ones. Meanwhile, our calculation of a three-arm junction with three main lanes and three secondary lanes is as follows:

$$TTT = \sum_{n=1}^{N} \int_0^T \int_{l_n}^{N} \rho(x,t)\, dx\, dt + \sum_{n=1}^{N} \int_0^T l_n(t)\, dt + T \cdot \sum_{n=1}^{N} \int_{l_n}^{N} \rho(x,T)\, dx + T \cdot \sum_{n=1}^{N} l_n(T) \tag{30}$$

$$TWT = \sum_{n=1}^{N} \int_0^T l_n(t)\, dt + T \cdot \sum_{n=1}^{N} l_n(T) \tag{31}$$

In addition, the efficiency of Total Travel Time and Total Waiting Time can be calculated by

$$TTT_{N1,L1}^{N2,L2} = \frac{(TTT_{L2}^{N2} - TTT_{L1}^{N1})}{TTT_{L1}^{N1}} \tag{32}$$

$$TWT_{N1,L1}^{N2,L2} = \frac{(TWT_{L2}^{N2} - TWT_{L1}^{N1})}{TWT_{L1}^{N1}} \tag{33}$$

where N is the number of arms and L refers to the circumference of the roundabout.

Results and Discussions

Validation

The numerous simulation results of Total Travel Time and Total Waiting Time on whole three-arm roundabouts are computed with the different values of F_{in}, β and P , as shown on Figures 7 and 8. The results of Total Travel Time and Total Waiting Time versus F_{in} are plotted with respect to β. The results can be compared with Obsu's paper, where the shape and properties are similar. However, the readings are higher than those in Obsu's results. This is because our simulation is based on three-arm junctions with six incoming roads and six outgoing roads on the roundabout while Obsu's study is simulated on an arm junction with two incoming roads and two outgoing roads.

Four-arm Roundabout

After the three-arm roundabout results have been validated, we extended our model to the four-arm roundabout. We plotted the Total Travel Time and Total Waiting Time results of the four-arm roundabout with three-unit and four-unit circumferences, as reflected in Figures 9 to 12. The results of three-arm and

four -arm roundabouts with the same three-unit circumference show that both Total Travel Time and Total Waiting Time readings have slightly increased because more cars entered the four-arm roundabout and it has a heavy density. On the contrary, when comparing the four-arm roundabout with three-unit and four-unit circumferences, it is found that the Total Travel Time reading has increased because of the increase in the travel distance. However, the Total Waiting Time reading has decreased because it has more spaces, and with a lower density.

Figure 13 shows the plot of Total Travel Time and Total Waiting Time of the four-arm roundabout with a four-unit circumference. In this case, the entry fluxes on the secondary lane are applied as $F_{\text{in}}^1 = 0.3, F_{\text{in}}^2 = 0.8, F_{\text{in}}^3 = 0.7$ and $F_{\text{in}}^4 = 0.5$. From this figure, it can be seen that the plot decreased as the β and P values increased. This is because the rates of exiting the roundabout and crossing the arm junction are increased, given the greater smoothness of traffic flow on the roundabout.

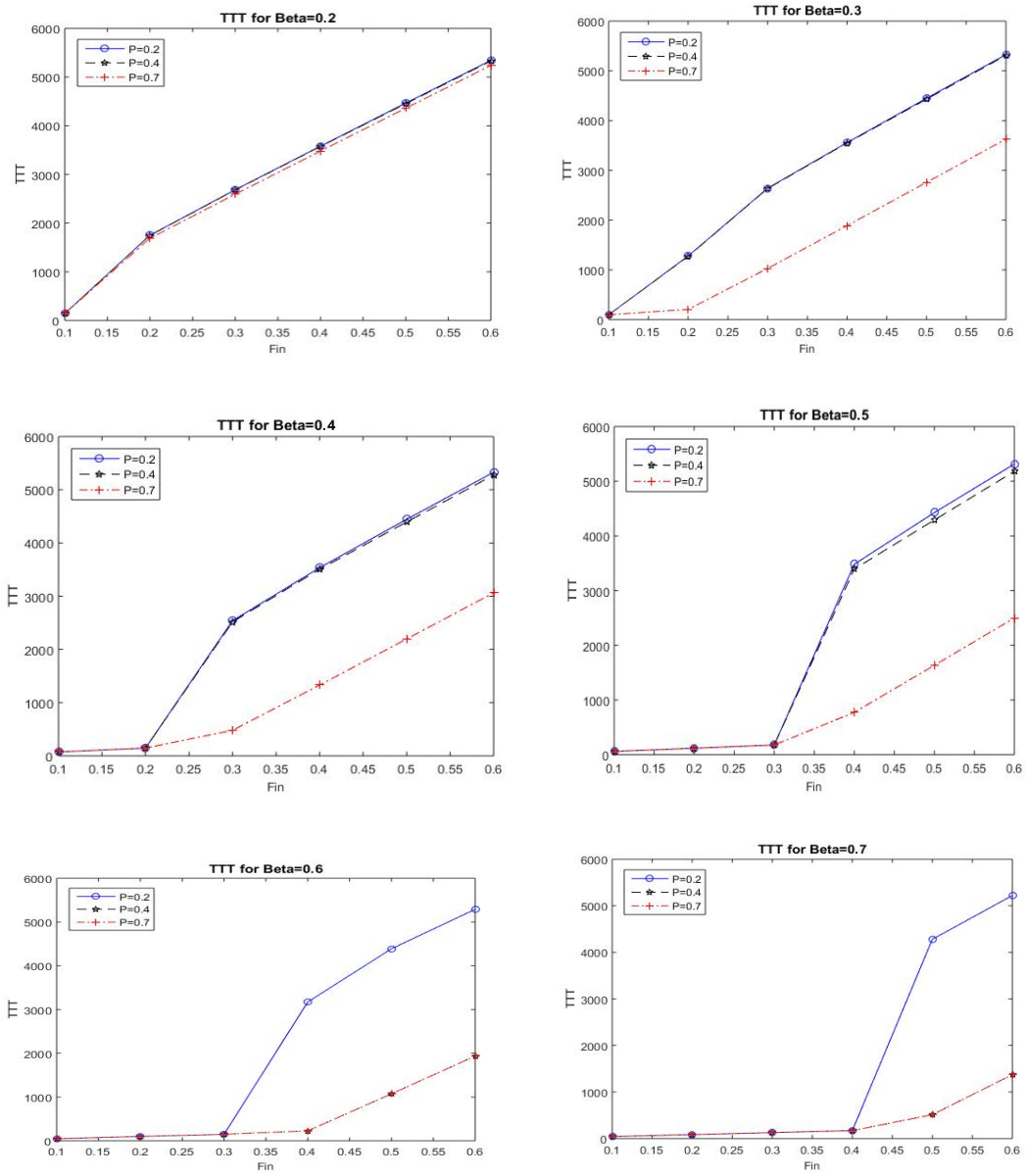

Figure 7. Plot of Total Travel Time versus F_{in} with various values of β for the three-arm roundabout with a 3-unit circumference.

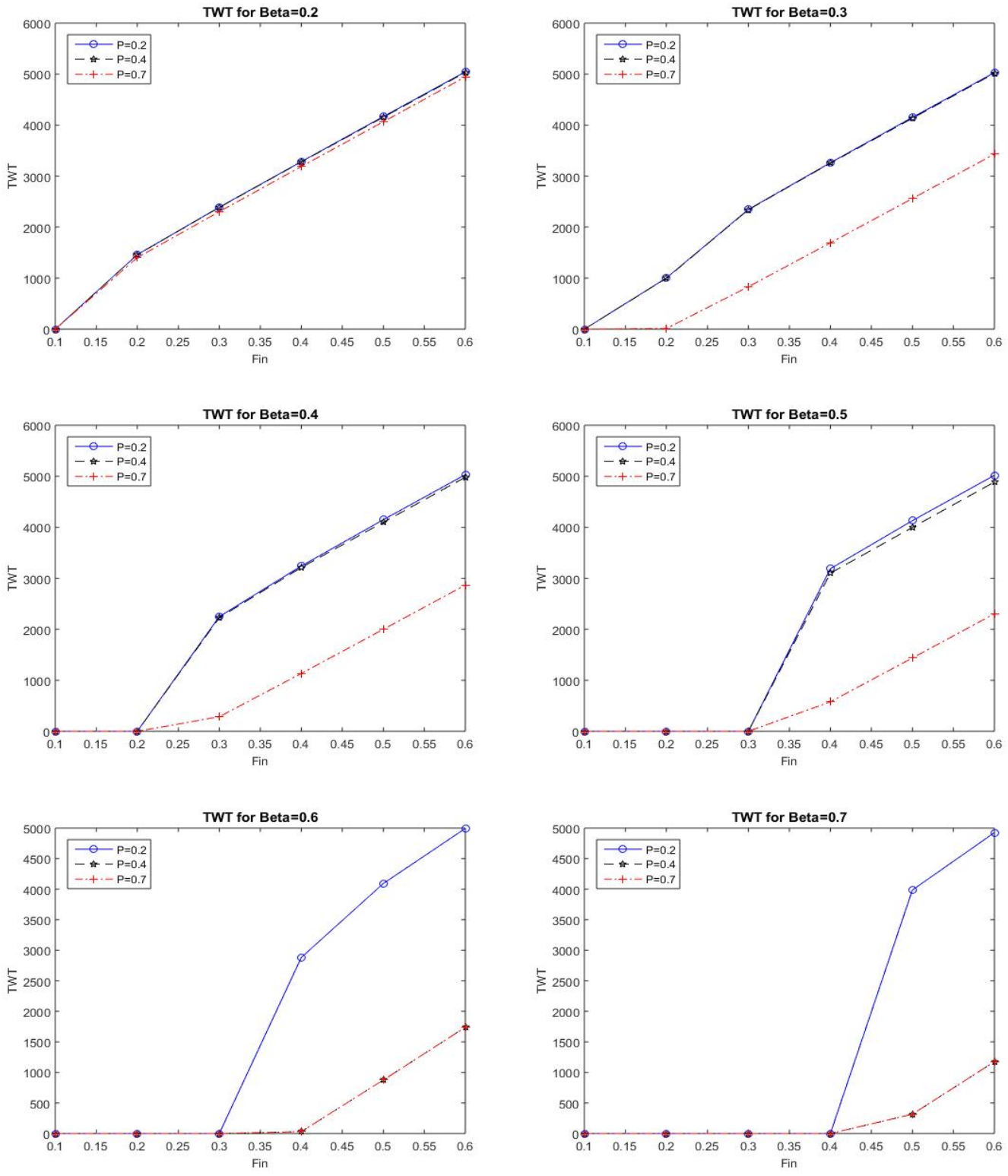

Figure 8. Plot of Total Waiting Time versus F_{in} with various values of β for the three-arm roundabout with a 3-unit circumference.

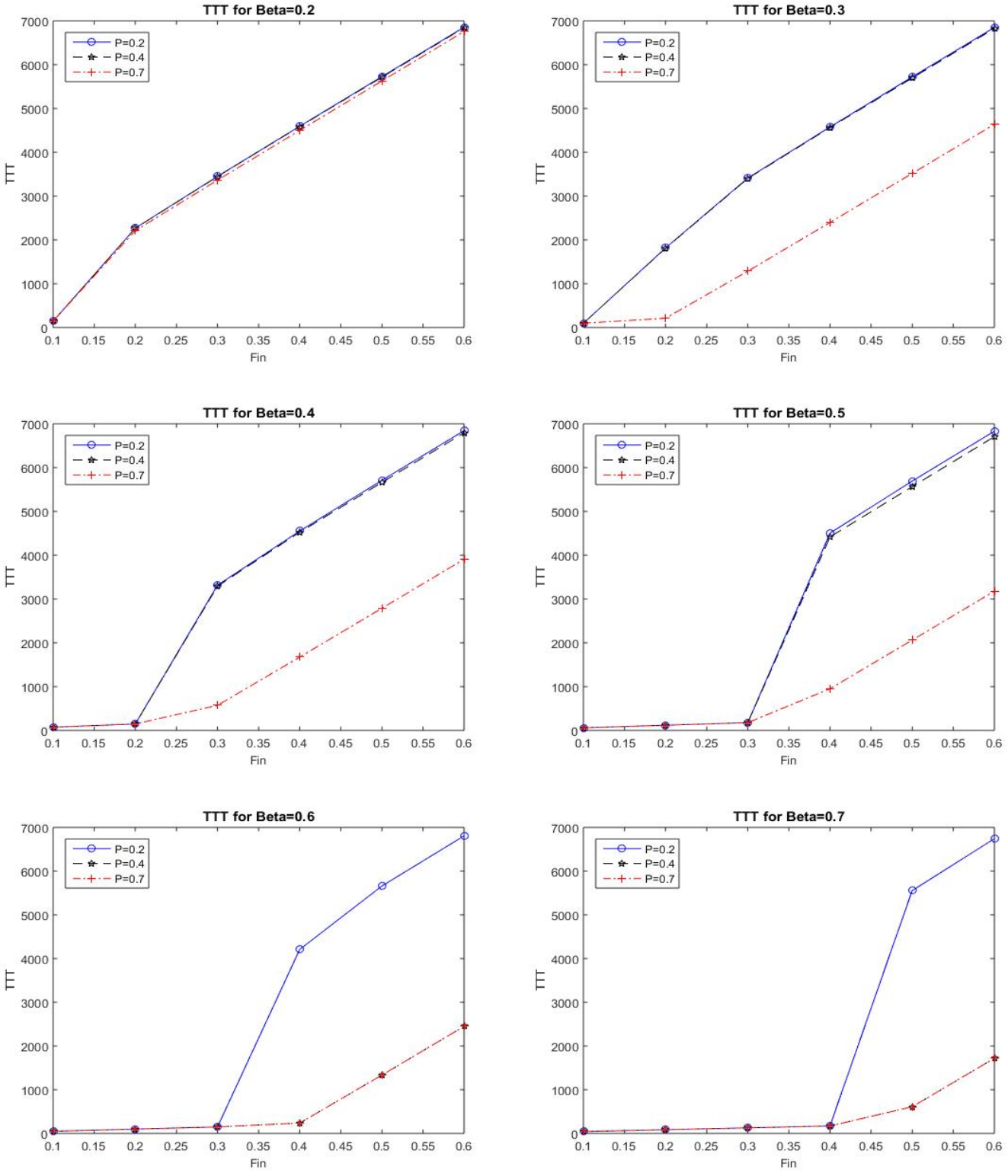

Figure 9. Plot of Total Travel Time versus F_{in} with various values of β for the four-arm roundabout with a 3-unit circumference.

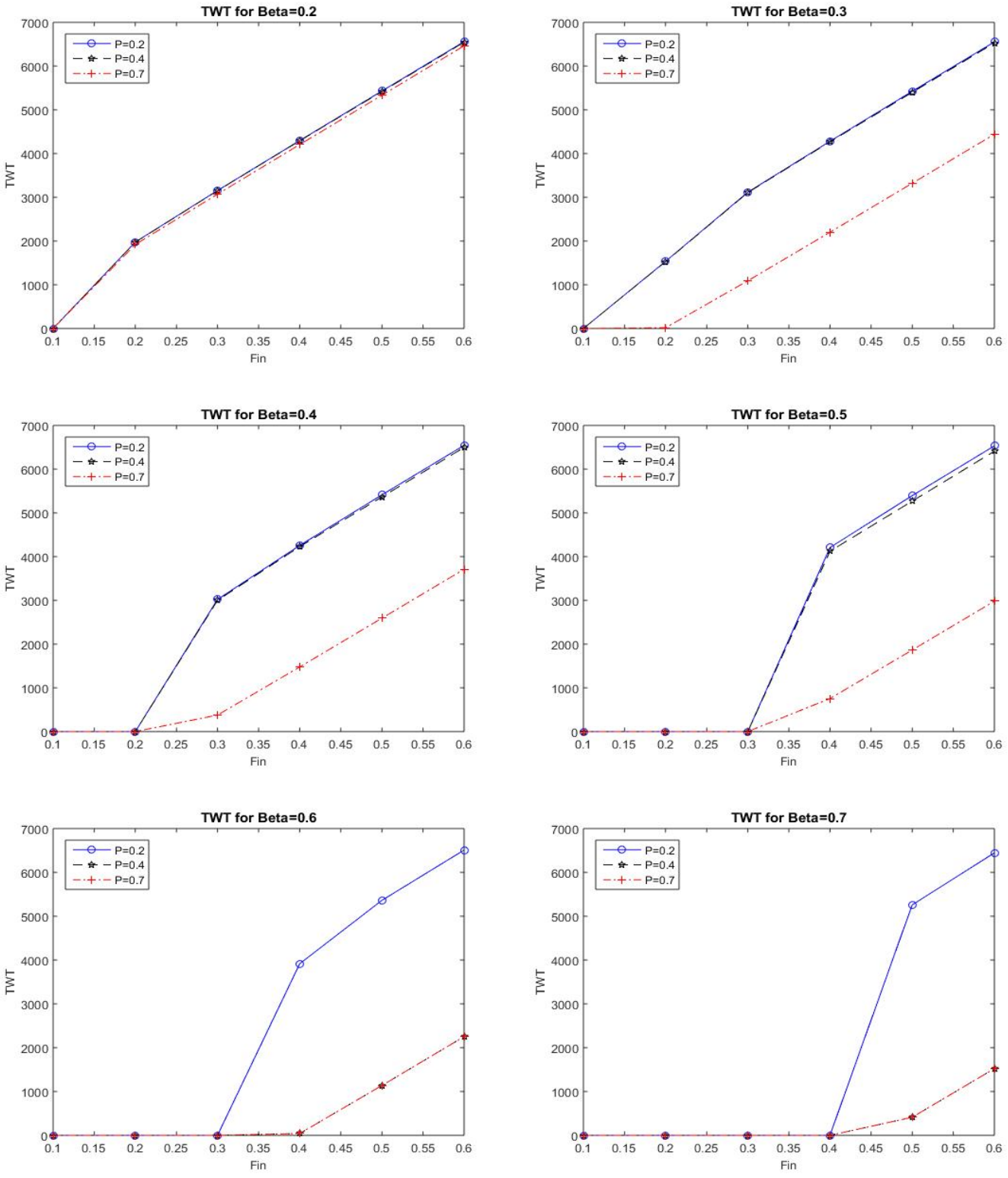

Figure 10. Plot of Total Waiting Time versus F_{in} with various values of β for the four-arm roundabout with a 3-unit circumference.

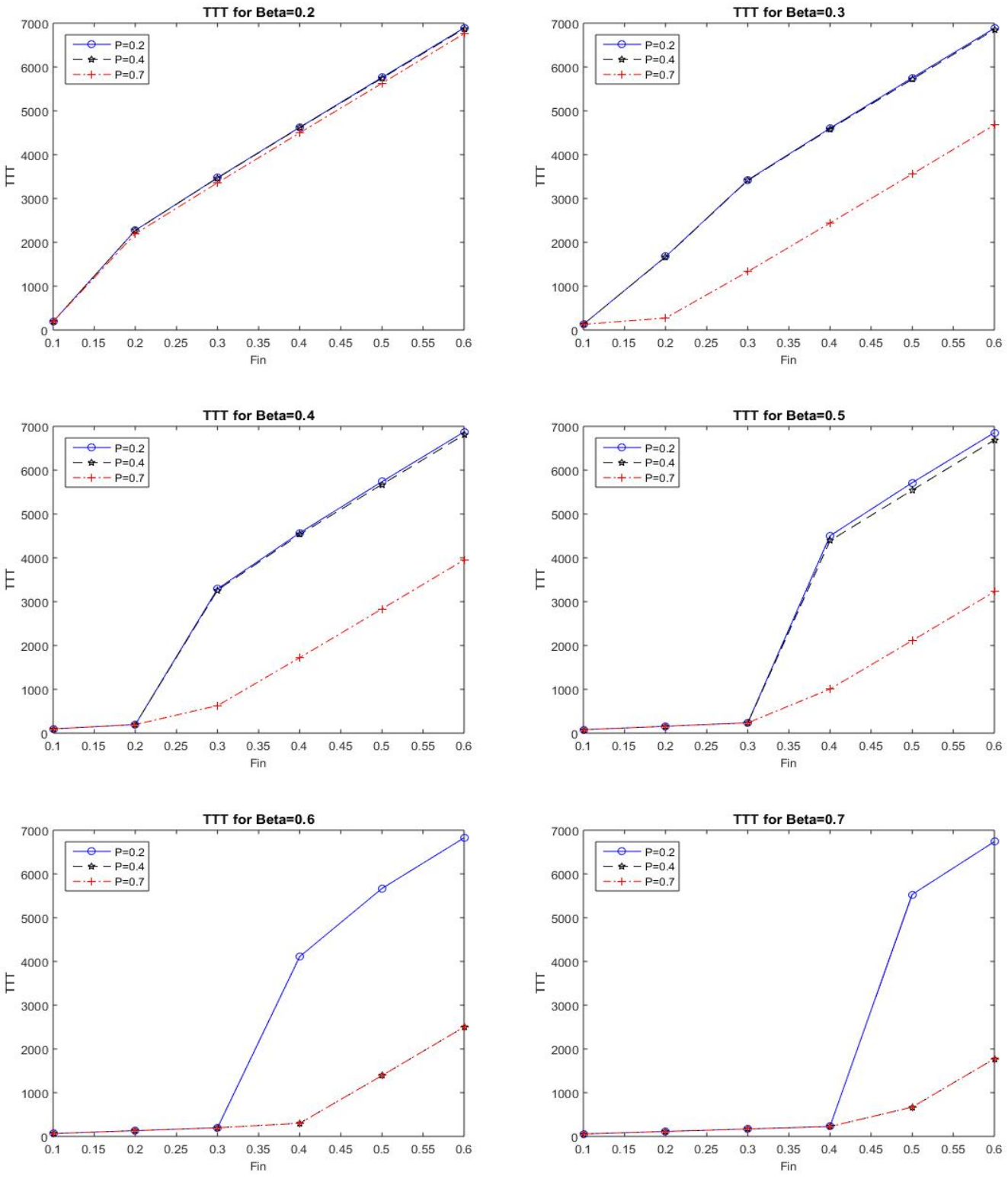

Figure 11. Plot of Total Travel Time versus F_{in} with various values of β for the four-arm roundabout with a 4-unit circumference.

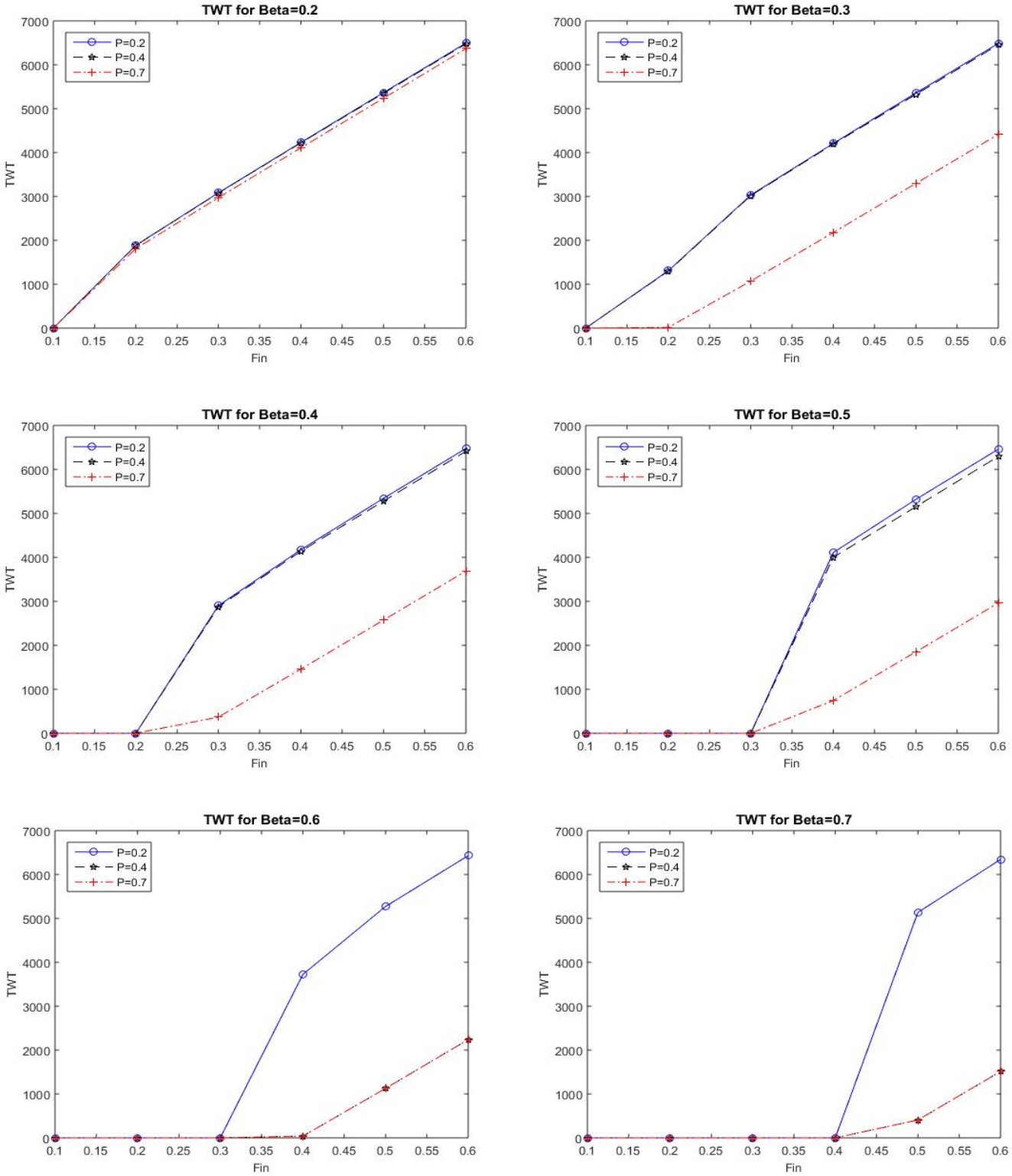

Figure 12. Plot of Total Waiting Time versus F_{in} with various values of β for four-arm roundabout with a 4-unit circumference.

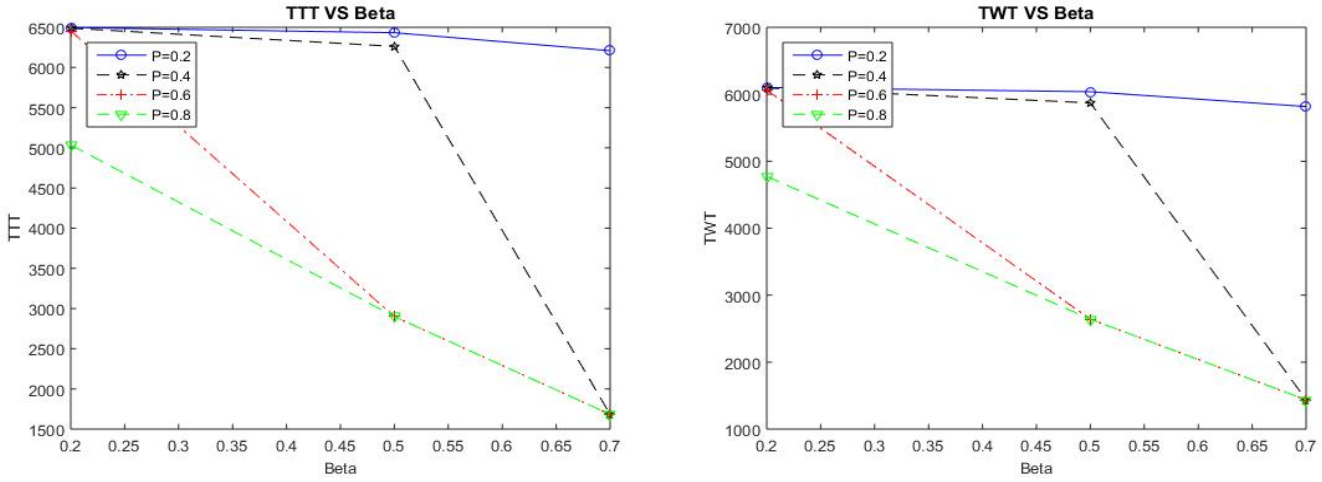

Figure 13. Plot of Total Travel Time and Total Waiting Time versus β for the four-arm roundabout with a 4-unit circumference where $F_{\text{in}}^1 = 0.3, F_{\text{in}}^2 = 0.8, F_{\text{in}}^3 = 0.7$ and $F_{\text{in}}^4 = 0.5$.

Queue Length

In addition, Figures 14 to 16 present the queue length on the incoming road of the secondary lane. Based on these figures, the queue length increased as the P value increased. The P value indicates the permissible rate for the flux crossing the arm junction. Hence, it reduced the flow from the secondary lane entering the roundabout. In this phenomenon, the β plays a very important role too, because when the rate of exiting the roundabout flow is increased, the heavy traffic on the main lane of the roundabout will reduce slightly, hence enabling an easier and greater traffic stream from the secondary lane to enter the roundabout. Thus, the queue length on the secondary lane is decreased.

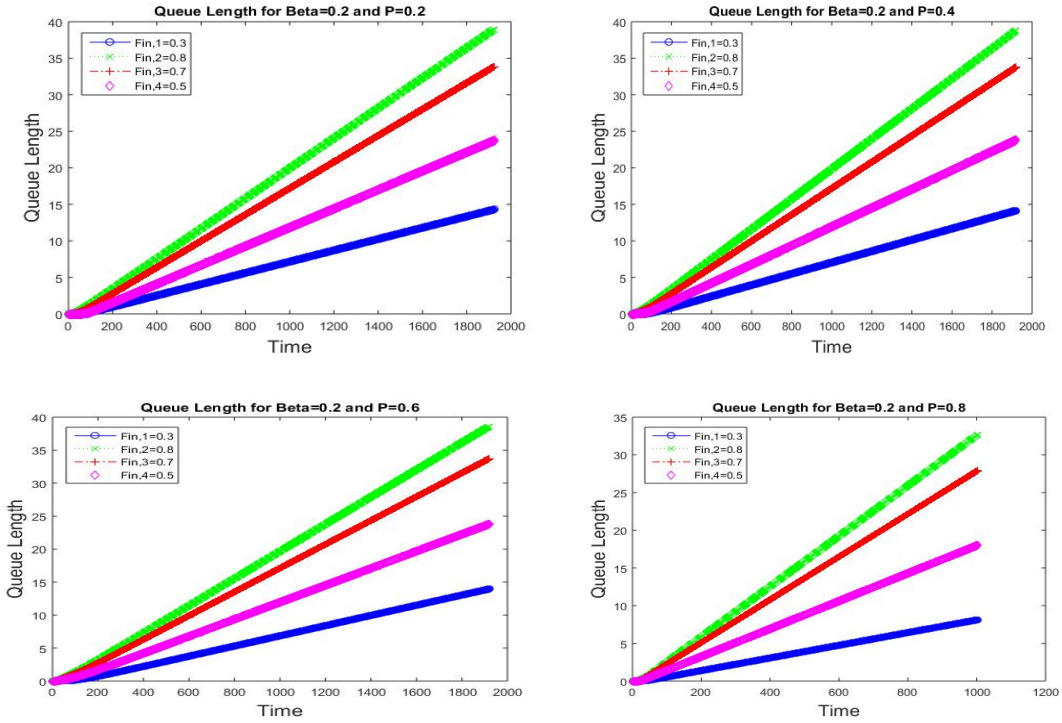

Figure 14. Plot of Queue Length for the four-arm roundabout with a 4-unit circumference where $F_{\text{in}}^1 = 0.3, F_{\text{in}}^2 = 0.8, F_{\text{in}}^3 = 0.7$ and $F_{\text{in}}^4 = 0.5$ for $\beta = 0.2$ and various values of P.

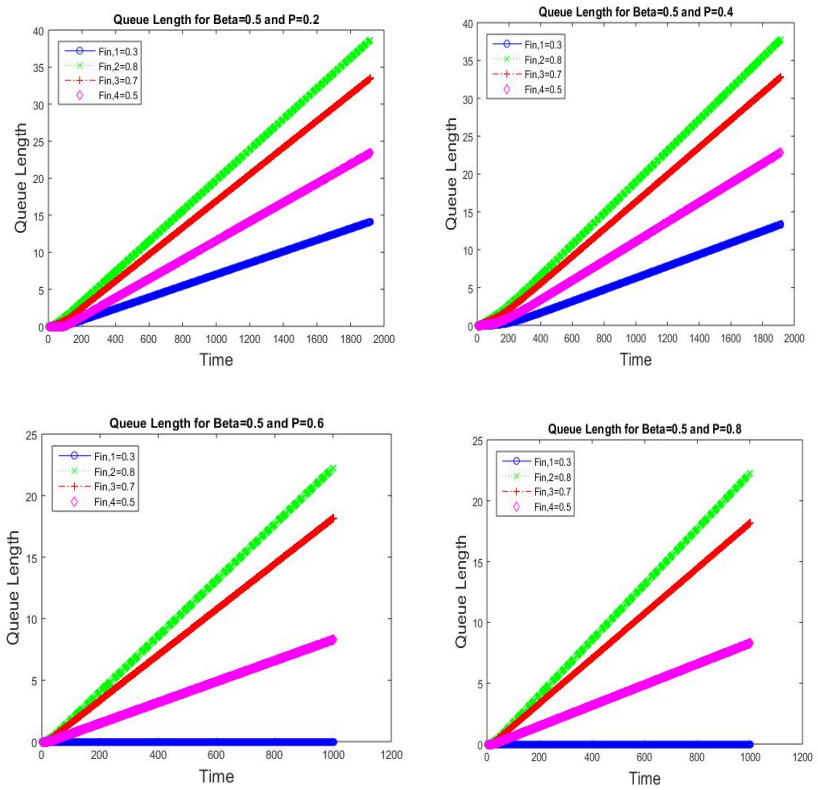

Figure 15. Plot of Queue Length for the four-arm roundabout with a 4-unit circumference where $F_{\text{in}}^1 = 0.3, F_{\text{in}}^2 = 0.8, F_{\text{in}}^3 = 0.7$ and $F_{\text{in}}^4 = 0.5$ for $\beta = 0.5$ and various values of P.

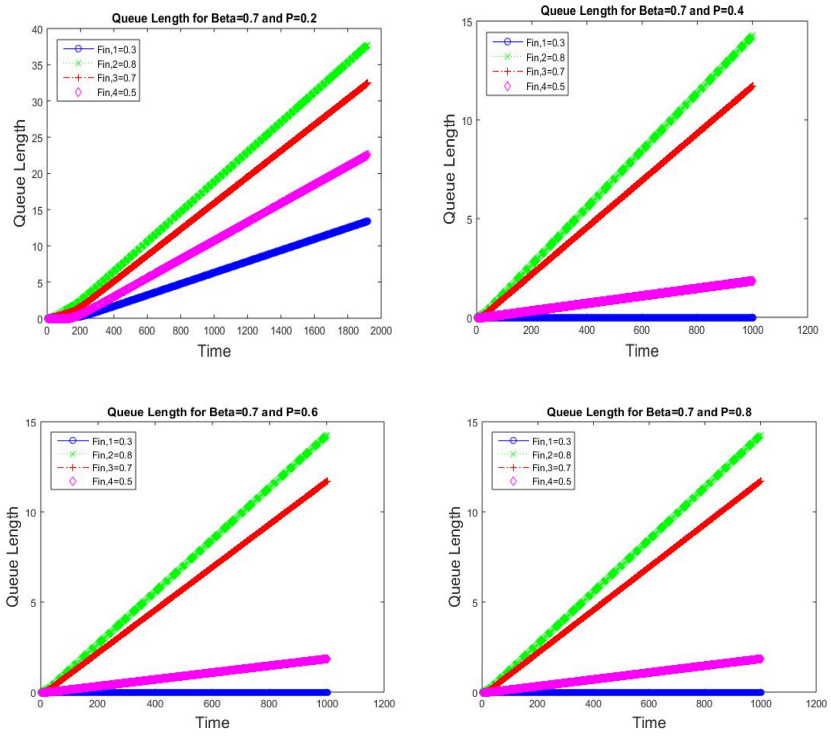

Figure 16. Plot of Queue Length for the four-arm roundabout with a 4-unit circumference where $F_{\text{in}}^1 = 0.3, F_{\text{in}}^2 = 0.8, F_{\text{in}}^3 = 0.7$ and $F_{\text{in}}^4 = 0.5$ for $\beta = 0.7$ and various values of P.

Density

Meanwhile, the different density plots of each road on the main lane are represented by Figures 17 to 19 for the three different values of $\beta = 0.2, 0.5, 0.7$ corresponded with $P = 0.2, 0.4, 0.6, 0.8$. Figure, 17 clearly demonstrates that when the crossing arm junction rate, P increased, the density on the roundabout became lower and traffic smoother. When the roundabout exiting rate β increased, the density on roundabout is also reduced, as shown in Figure 19.

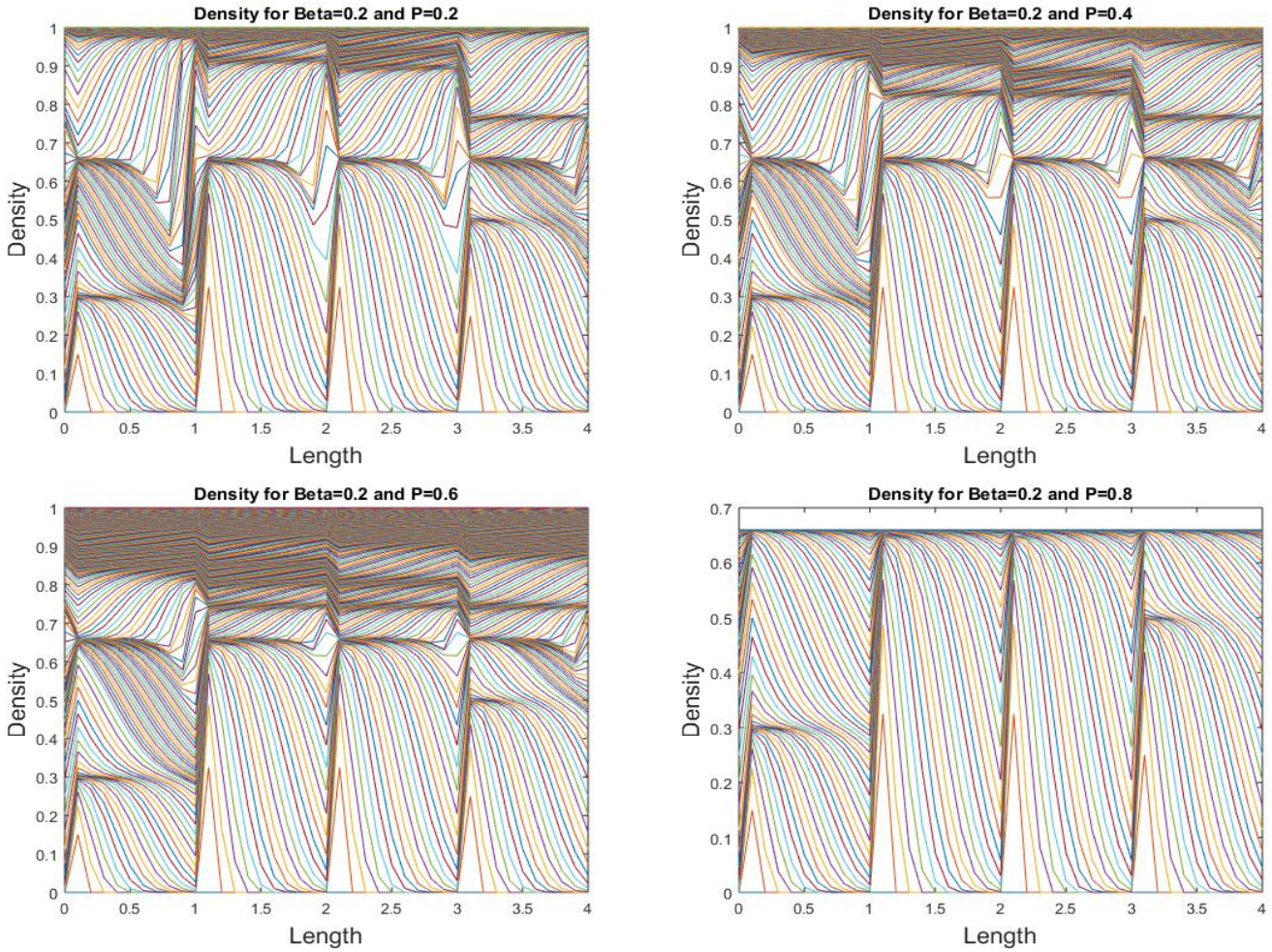

Figure 17. Plot of Density for the four-arm roundabout with a 4-unit circumference where $F_{\text{in}}^1 = 0.3, F_{\text{in}}^2 = 0.8, F_{\text{in}}^3 = 0.7$ and $F_{\text{in}}^4 = 0.5$ for $\beta = 0.2$ and various values of P.

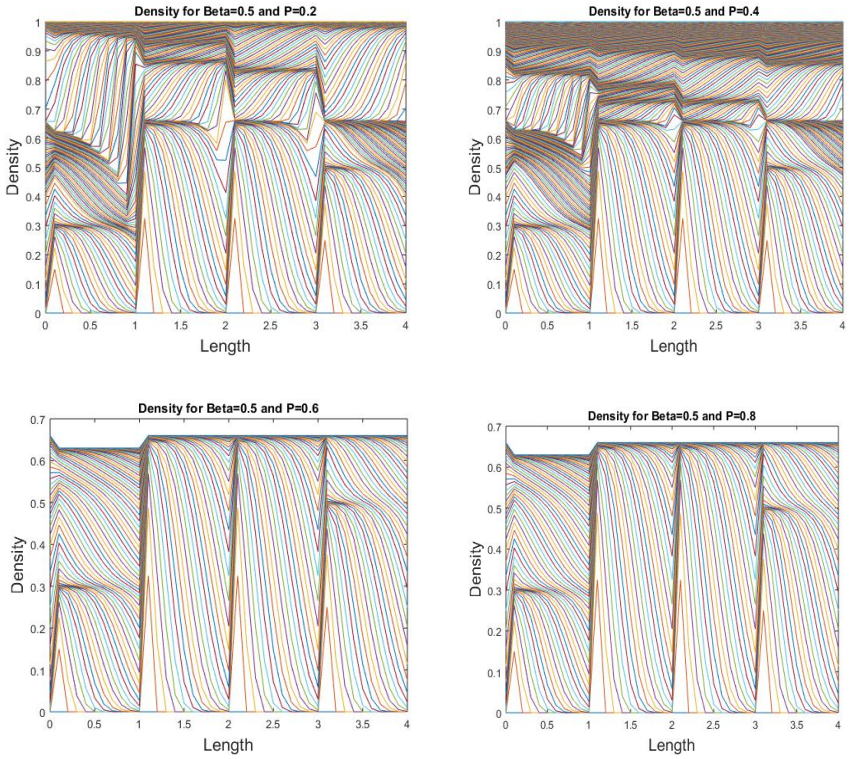

Figure 18. Plot of Density for the four-arm roundabout with a 4-unit circumference where $F_{\text{in}}^1 = 0.3, F_{\text{in}}^2 = 0.8, F_{\text{in}}^3 = 0.7$ and $F_{\text{in}}^4 = 0.5$ for $\beta = 0.5$ and various values of P.

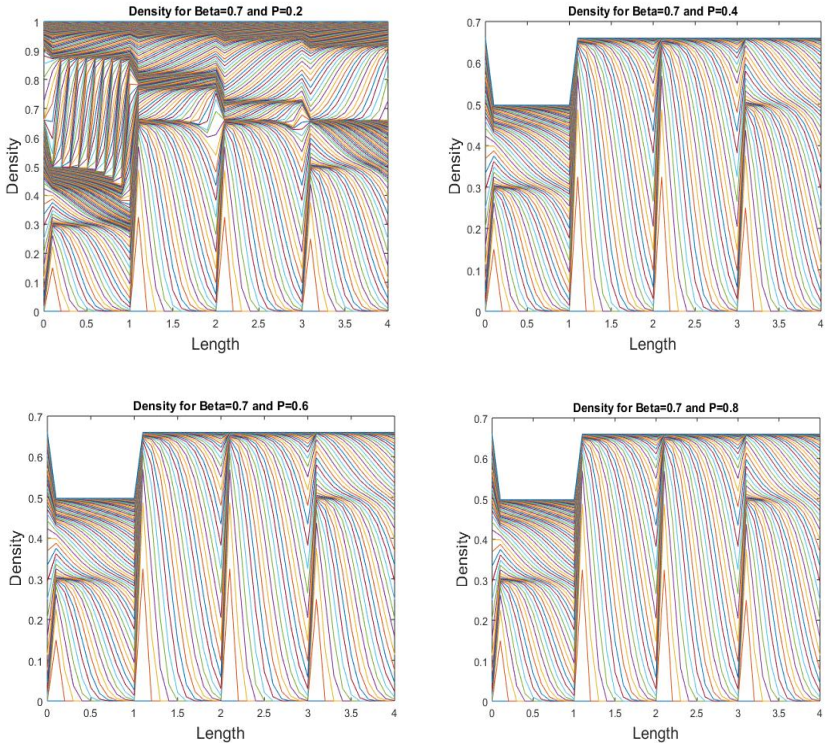

Figure 19. Plot of Density for the four-arm roundabout with a 4-unit circumference where $F_{\text{in}}^1 = 0.3, F_{\text{in}}^2 = 0.8, F_{\text{in}}^3 = 0.7$ and $F_{\text{in}}^4 = 0.5$ for $\beta = 0.7$ and various values of P.

Flexibility of Roundabout

Lastly, the Figure 20 shows the density and queue length plots for the different F_{in}, β and P on each arm junction. In Figure 20 (a), the density in between the length of one unit and two units is higher because the flux applied on the second arm is the highest value $F_{\text{in}}^2 = 0.8$ among the four arms. On the other hand, the density in between the length of zero unit and one unit is the lowest because the flux applied on first arm $F_{\text{in}}^1 = 0.3$ is the smallest value. Moreover, the roundabout exiting rate on the second arm is high, $\beta_2 = 0.7$. In Figure 20 (b), the queue length on the third arm is the longest because the flux applied on the third arm is $F_{\text{in}}^3 = 0.7$; the crossing arm junction flux rate $P_3 = 0.4$ and exiting the roundabout on the fourth arm has the lowest rate $\beta_4 = 0.2$. It prevents the cars on the third arm from entering the roundabout, hence leading to an increase in the queue length. Even though the F_{in}^2 is the highest rate, the roundabout exiting rate is low, $P_2 = 0.7$. The roundabout exiting rate is high enough on the third arm, $\beta_3 = 0.8$. So, the queue on the second arm is not the longest but is the second in place, among the four arms. The queue length on the first arm is the shortest because $F_{\text{in}}^1 = 0.3$ is the lowest rate, and the roundabout exiting rate on the second arm is considered high, $\beta_2 = 0.7$.

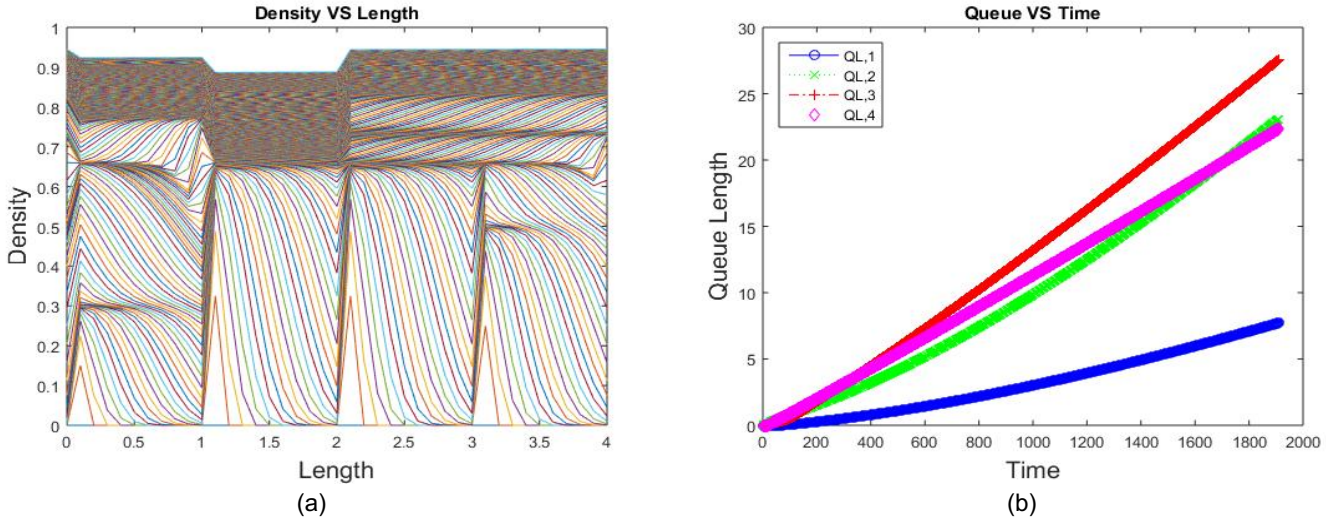

Figure 20. Plot of the four-arm roundabout with a 4-unit circumference where $F_{\text{in}}^1 = 0.3, F_{\text{in}}^2 = 0.8, F_{\text{in}}^3 = 0.7$, $F_{\text{in}}^4 = 0.5$, $\beta_1 = 0.3$, $\beta_2 = 0.7$, $\beta_3 = 0.8$, $\beta_4 = 0.2$, $P_1 = 0.5$, $P_2 = 0.2$, $P_3 = 0.4$, and $P_4 = 0.8$. (a) Density versus Length. (b) Queue versus Time.

Efficiency

Tables 1 to 12 describe the efficiency between three-arm roundabout and four-arm roundabout with various values of β and P for the 3-unit circumference and 4-unit circumference. The overall results explained the efficiency for the expansion from three-arm roundabout to four-arm roundabout as well as the increment of the circumference of roundabout from 3-unit circumference to 4-unit circumference.

Table 1. Efficiency of three arms versus four arms with a 3-unit circumference for $\beta = 0.2$.

F_{in}	$P = 0.2$		$P = 0.4$		$P = 0.7$	
	$TTT_{3,3}^{4,3}$	$TWT_{3,3}^{4,3}$	$TTT_{3,3}^{4,3}$	$TWT_{3,3}^{4,3}$	$TTT_{3,3}^{4,3}$	$TWT_{3,3}^{4,3}$
0.1	1.1725%	0.0000%	1.1725%	0.0000%	1.1725%	0.0000%
0.2	29.6191%	35.3086%	29.6796%	35.3740%	30.8608%	36.9588%
0.3	28.4922%	31.9351%	28.5464%	31.9997%	29.6789%	33.3131%
0.4	28.3244%	30.8423%	28.3772%	30.9032%	29.2894%	31.9052%
0.5	28.2969%	30.2923%	28.3968%	30.3995%	29.1162%	31.1673%
0.6	28.3201%	29.9744%	28.4007%	30.0616%	28.9820%	30.6675%

Table 2. Efficiency of three arms vs four arms with a 3-unit circumference for $\beta = 0.3$.

F_{in}	$P = 0.2$		$P = 0.4$		$P = 0.7$	
	$TTT_{3,3}^{4,3}$	$TWT_{3,3}^{4,3}$	$TTT_{3,3}^{4,3}$	$TWT_{3,3}^{4,3}$	$TTT_{3,3}^{4,3}$	$TWT_{3,3}^{4,3}$
0.1	0.7227%	0.0000%	0.7227%	0.0000%	0.7227%	0.0000%
0.2	42.0797%	53.0456%	42.2826%	53.3691%	3.2033%	42.0071%
0.3	29.1821%	32.7498%	29.1494%	32.7255%	25.1971%	31.0433%
0.4	28.6357%	31.1922%	28.6093%	31.1713%	26.9656%	30.0679%
0.5	28.6052%	30.6210%	28.5608%	30.5815%	27.5328%	29.6345%
0.6	28.5964%	30.2644%	28.5222%	30.1906%	27.8144%	29.4006%

Table 3. Efficiency of three arms vs four arms with a 3-unit circumference for $\beta = 0.4$.

F_{in}	$P = 0.2$		$P = 0.4$		$P = 0.7$	
	$TTT_{3,3}^{4,3}$	$TWT_{3,3}^{4,3}$	$TTT_{3,3}^{4,3}$	$TWT_{3,3}^{4,3}$	$TTT_{3,3}^{4,3}$	$TWT_{3,3}^{4,3}$
0.1	0.5041%	0.0000%	0.5041%	0.0000%	0.5041%	0.0000%
0.2	0.5039%	0.0000%	0.5039%	0.0000%	0.5039%	0.0000%
0.3	30.5075%	34.3622%	30.8129%	34.7281%	19.2021%	32.0774%
0.4	28.7504%	31.3326%	29.0363%	31.6602%	25.8137%	30.2442%
0.5	28.4461%	30.4575%	28.8465%	30.8997%	27.0347%	29.6784%
0.6	28.4090%	30.0725%	28.7482%	30.4367%	27.5272%	29.4058%

Table 4. Efficiency of three arms vs four arms with a 3-unit circumference for $\beta = 0.5$.

F_{in}	$P = 0.2$		$P = 0.4$		$P = 0.7$	
	$TTT_{3,3}^{4,3}$	$TWT_{3,3}^{4,3}$	$TTT_{3,3}^{4,3}$	$TWT_{3,3}^{4,3}$	$TTT_{3,3}^{4,3}$	$TWT_{3,3}^{4,3}$
0.1	0.3745%	0.0000%	0.3745%	0.0000%	0.3745%	0.0000%
0.2	0.3745%	0.0000%	0.3745%	0.0000%	0.3745%	0.0000%
0.3	0.3744%	0.0000%	0.3744%	0.0000%	0.3744%	0.0000%
0.4	29.3369%	31.9991%	30.1750%	32.9722%	22.9021%	30.5867%
0.5	28.5924%	30.6228%	29.6640%	31.8123%	26.1905%	29.7433%
0.6	28.4935%	30.1658%	29.4353%	31.1825%	27.1186%	29.4222%

Table 5. Efficiency of three arms vs four arms with a 3-unit circumference for $\beta = 0.6$.

F_{in}	$P = 0.2$		$P = 0.4$		$P = 0.7$	
	$TTT_{3,3}^{4,3}$	$TWT_{3,3}^{4,3}$	$TTT_{3,3}^{4,3}$	$TWT_{3,3}^{4,3}$	$TTT_{3,3}^{4,3}$	$TWT_{3,3}^{4,3}$
0.1	0.2888%	0.0000%	0.2888%	0.0000%	0.2888%	0.0000%
0.2	0.2889%	0.0000%	0.2889%	0.0000%	0.2889%	0.0000%
0.3	0.2888%	0.0000%	0.2888%	0.0000%	0.2888%	0.0000%
0.4	32.6713%	35.8794%	4.7439%	32.9437%	4.7439%	32.9437%
0.5	28.9432%	31.0089%	24.4382%	29.8800%	24.4382%	29.8800%
0.6	28.6559%	30.3424%	26.4653%	29.4419%	26.4653%	29.4419%

Table 6. Efficiency of three arms vs four arms with a 3-unit circumference for $\beta = 0.7$.

F_{in}	$P = 0.2$		$P = 0.4$		$P = 0.7$	
	$TTT_{3,3}^{4,3}$	$TWT_{3,3}^{4,3}$	$TTT_{3,3}^{4,3}$	$TWT_{3,3}^{4,3}$	$TTT_{3,3}^{4,3}$	$TWT_{3,3}^{4,3}$
0.1	0.2280%	0.0000%	0.2280%	0.0000%	0.2280%	0.0000%
0.2	0.2282%	0.0000%	0.2282%	0.0000%	0.2282%	0.0000%
0.3	0.2280%	0.0000%	0.2280%	0.0000%	0.2280%	0.0000%
0.4	0.2280%	0.0000%	0.2280%	0.0000%	0.2280%	0.0000%
0.5	29.7592%	31.9275%	18.7505%	30.2723%	18.7505%	30.2723%
0.6	29.1087%	30.8376%	25.2641%	29.4668%	25.2641%	29.4668%

Table 7. Efficiency of four arms with a 3-unit circumference vs a 4-unit circumference for $\beta = 0.2$.

F_{in}	$P = 0.2$		$P = 0.4$		$P = 0.7$	
	$TTT_{4,3}^{4,4}$	$TWT_{4,3}^{4,4}$	$TTT_{4,3}^{4,4}$	$TWT_{4,3}^{4,4}$	$TTT_{4,3}^{4,4}$	$TWT_{4,3}^{4,4}$
0.1	31.7881%	0.0000%	31.7881%	0.0000%	31.7881%	0.0000%
0.2	0.1939%	-4.5261%	0.1544%	-4.5678%	-0.6786%	-5.5981%
0.3	0.6927%	-2.3045%	0.6529%	-2.3487%	-0.1516%	-3.2400%
0.4	0.6596%	-1.5664%	0.6212%	-1.6055%	-0.0289%	-2.2970%
0.5	0.5867%	-1.1897%	0.5144%	-1.2643%	-0.0036%	-1.7982%
0.6	0.5062%	-0.9714%	0.4471%	-1.0312%	0.0311%	-1.4543%

Table 8. Efficiency of four arms with a 3-unit circumference vs a 4-unit circumference for $\beta = 0.3$.

F_{in}	$P = 0.2$		$P = 0.4$		$P = 0.7$	
	$TTT_{4,3}^{4,4}$	$TWT_{4,3}^{4,4}$	$TTT_{4,3}^{4,4}$	$TWT_{4,3}^{4,4}$	$TTT_{4,3}^{4,4}$	$TWT_{4,3}^{4,4}$
0.1	32.3766%	0.0000%	32.3766%	0.0000%	32.3766%	0.0000%
0.2	-7.8472%	-14.8841%	-7.9717%	-15.0562%	28.9787%	-8.6879%
0.3	0.3195%	-2.7337%	0.2351%	-2.8315%	3.5836%	-1.6966%
0.4	0.5461%	-1.6936%	0.4600%	-1.7873%	1.7640%	-1.0357%
0.5	0.5437%	-1.2337%	0.3986%	-1.3874%	1.1600%	-0.7349%
0.6	0.4817%	-0.9981%	0.3633%	-1.1197%	0.8581%	-0.5742%

Table 9. Efficiency of four arms with a 3-unit circumference vs a 4-unit circumference for $\beta = 0.4$.

F_{in}	$P = 0.2$		$P = 0.4$		$P = 0.7$	
	$TTT_{4,3}^{4,4}$	$TWT_{4,3}^{4,4}$	$TTT_{4,3}^{4,4}$	$TWT_{4,3}^{4,4}$	$TTT_{4,3}^{4,4}$	$TWT_{4,3}^{4,4}$
0.1	32.6647%	0.0000%	32.6647%	0.0000%	32.6647%	0.0000%
0.2	32.6648%	0.0000%	32.6648%	0.0000%	32.6648%	0.0000%
0.3	-0.7060%	-3.9159%	-0.9138%	-4.1556%	9.6514%	-2.3965%
0.4	0.3625%	-1.8963%	0.1591%	-2.1190%	2.8619%	-1.1509%
0.5	0.4817%	-1.3027%	0.1996%	-1.6050%	1.6241%	-0.7638%
0.6	0.4443%	-1.0375%	0.2046%	-1.2899%	1.1233%	-0.5793%

Table 10. Efficiency of four arms with a 3-unit circumference vs a 4-unit circumference for $\beta = 0.5$.

F_{in}	$P = 0.2$		$P = 0.4$		$P = 0.7$	
	$TTT_{4,3}^{4,4}$	$TWT_{4,3}^{4,4}$	$TTT_{4,3}^{4,4}$	$TWT_{4,3}^{4,4}$	$TTT_{4,3}^{4,4}$	$TWT_{4,3}^{4,4}$
0.1	32.8358%	0.0000%	32.8358%	0.0000%	32.8358%	0.0000%
0.2	32.8359%	0.0000%	32.8359%	0.0000%	32.8359%	0.0000%
0.3	32.8360%	0.0000%	32.8360%	0.0000%	32.8360%	0.0000%
0.4	-0.0488%	-2.3503%	-0.6269%	-2.9998%	5.7139%	-1.3881%
0.5	0.3778%	-1.4145%	-0.3720%	-2.2263%	2.4252%	-0.8097%
0.6	0.3836%	-1.1022%	-0.2818%	-1.8050%	1.5038%	-0.5870%

Table 11. Efficiency of four arms with a 3-unit circumference vs a 4-unit circumference for $\beta = 0.6$.

F_{in}	$P = 0.2$		$P = 0.4$		$P = 0.7$	
	$TTT_{4,3}^{4,4}$	$TWT_{4,3}^{4,4}$	$TTT_{4,3}^{4,4}$	$TWT_{4,3}^{4,4}$	$TTT_{4,3}^{4,4}$	$TWT_{4,3}^{4,4}$
0.1	32.9492%	0.0000%	32.9492%	0.0000%	32.9492%	0.0000%
0.2	32.9492%	0.0000%	32.9492%	0.0000%	32.9492%	0.0000%
0.3	32.9493%	0.0000%	32.9493%	0.0000%	32.9493%	0.0000%
0.4	-2.3122%	-4.8934%	26.7273%	-2.9746%	26.7273%	-2.9746%
0.5	0.1308%	-1.6823%	4.1061%	-0.9053%	4.1061%	-0.9053%
0.6	0.2703%	-1.2244%	2.1151%	-0.5995%	2.1151%	-0.5995%

Table 12. Efficiency of four arms with a 3-unit circumference vs 4-unit circumference for $\beta = 0.7$.

F_{in}	$P = 0.2$		$P = 0.4$		$P = 0.7$	
	$TTT_{4,3}^{4,4}$	$TWT_{4,3}^{4,4}$	$TTT_{4,3}^{4,4}$	$TWT_{4,3}^{4,4}$	$TTT_{4,3}^{4,4}$	$TWT_{4,3}^{4,4}$
0.1	33.0300%	0.0000%	33.0300%	0.0000%	33.0300%	0.0000%
0.2	33.0299%	0.0000%	33.0299%	0.0000%	33.0299%	0.0000%
0.3	33.0300%	0.0000%	33.0300%	0.0000%	33.0300%	0.0000%
0.4	33.0299%	0.0000%	33.0299%	0.0000%	33.0299%	0.0000%
0.5	-0.4321%	-2.2991%	9.8953%	-1.1731%	9.8953%	-1.1731%
0.6	-0.0460%	-1.5641%	3.2509%	-0.6240%	3.2509%	-0.6240%

Conclusions

The modeling of the three-arm roundabout, based on macroscopic and hyperbolic conservation laws, is created and validated with Obsu's model. Subsequently, the model is expanded to the four-arm roundabout. In our model, there are many adjustable parameters, F_{in}, β and P, on each arm of the roundabout. Therefore, our model is flexible and is capable of operating like a real phenomenon. As mentioned in the results and discussion section, the findings generated in terms of Total Travel Time and Total Waiting Time show that the density and queue length are reasonable and logical. Finally, it has led us to study the performance and efficiency of the roundabout where the data in Tables 1 to 12 reflect the efficiency percentage of the roundabout in both the three-arm and four-arm roundabouts with several parameters.

Acknowledgments

This research is fully supported by Research Management Center, Universiti Teknologi Malaysia (UTM) for the Collaborative Research Grant (R.J130000.7354.4B506). The support is gratefully acknowledged.

References

[1] G. R. Iordanidou, I. Papamichail, C. Roncoli and M. Papageorgion, "Feedback-Based Integrated Motorway Traffic Flow Control with Delay Balancing," IEEE Transactions on Intelligent Transportation Systems, vol. 18, no. 9, pp. 2319–2329, 2017.

[2] R. Wang and H. J. Ruskin, "Modeling traffic flow at a single-lane urban roundabout," Computer Physics Communications, vol. 147, pp. 570–576, 2002.

[3] L. L. Obsu, M. L. D. Monache, P. Goatin and S. M. Kassa, "Traffic flow optimization on roundabouts," Mathematical Methods in the Applied Sciences, vol. 38, no. 14, pp. 3075–3096, 2015.

[4] S. Daniel, "A Simulation of Road Traffic to Model Causes of Congestion," The University of Bath: Bachelor's Thesis, 2009.

[5] C. F. Daganzo, "A finite difference approximation of the kinematic wave model of traffic flow," Transportation Research Part B: Methodological, vol. 29, no. 4, pp. 261-276, 1995.

[6] E. Sonnendrucker, "Numerical methods for hyperbolic systems," Lecture Notes, 2013.

[7] V. Mukundan and A. Awasthi, "Efficient numerical techniques for Burgers' equation," Applied Mathematics and Computation, vol. 262, pp. 282–297, 2015.

[8] M. L. D. Monache, "Traffic flow modeling by Conservation Laws," University Nice Sophia Antipolis: Ph.D. Thesis, 2014.

[9] M. L. D. Monache, S. Samaranayake, J. Reilly et al., "A PDE-ODE for a Junction with Ramp Buffer," SIAM Journal on Applied Mathematics, vol. 74, pp. 22-39, 2014.